PHYSICAL REVIEW D
PARTICLES AND FIELDS

THIRD SERIES, VOLUME 39, NUMBER 9 — 1 MAY 1989

Recoil-proton polarization in πp elastic scattering at 547 and 625 MeV/c

C. J. Seftor, S. D. Adrian, W. J. Briscoe, A. Mokhtari, and M. F. Taragin
Department of Physics, The George Washington University, Washington, D.C. 20052

M. E. Sadler
Department of Physics, Abilene Christian University, Abilene, Texas 79699

D. B. Barlow, B. M. K. Nefkens, and C. Pillai
Department of Physics, University of California, Los Angeles, California 90024

(Received 6 October 1988)

The polarization of the recoil proton in π^+p and π^-p elastic scattering using a liquid-hydrogen target has been measured for backward angles at 547 and 625 MeV/c. The scattered pion and recoil proton were detected in coincidence using the large-acceptance spectrometer to detect and analyze the momentum of the pions and the JANUS polarimeter to identify and measure the polarization of the protons. Results from this experiment agree with other measurements of the recoil polarization, with analyzing-power data previously taken by this group, and with predictions of partial-wave analyses.

I. INTRODUCTION

One of the simplest hadronic systems that can be studied experimentally is the pion-nucleon (πN) system. The πN interaction is of particular interest since the long-range part of the nucleon-nucleon (NN) interaction is easily explained in terms of π exchange. Many strong-interaction models (based on an underlying QCD structure) have been developed in an attempt to explain low-energy πN interactions.[1-14] These models differ in their predictions of the masses and widths of several of the hadronic resonances. To test these models, comparisons are made to the resonances emanating from the πN scattering amplitudes as determined by partial-wave analysis (PWA). In turn these PWA's are themselves tested by comparison of the observables calculated from these amplitudes to new experimental data. The subsequent inclusion of these experimental results in the data base used in the PWA's leads to a more accurate set of πN amplitudes.

The determination of a complete and unambiguous set of πN amplitudes requires measurement of four independent observables for each energy and angle:[15] the differential cross section $d\sigma/d\Omega$, the polarization P (or, from the $P=A_n$ theorem, the analyzing power A_n), and the spin-rotation parameters A and R. Since a complete set of experimental data is not available in the resonance region, ambiguities arise in the PWA's which are resolved by imposing theoretical constraints.

The three major PWA's available for the πN system have been produced by Carnegie Mellon University–Lawrence Berkeley Laboratory[16] (CMU-LBL), Karlsruhe-Helsinki[17] (KH), and Virginia Polytechnic Institute[18] (VPI). The difference among these PWA's lies in the application of theoretical constraints and in the data base each uses. The KH and CMU-LBL data bases are rather old and their analyses rely on the use of dispersion relations to resolve ambiguities, while the VPI analysis uses an ansatz for the variation of the scattering amplitudes and has a carefully updated data base. The different approaches among the PWA's lead to disagreement in the number of resonances, their masses, and their widths. Of particular interest is the P_{11}(Roper) resonance at 1440 MeV. The VPI group, which characterizes resonances in terms of pole positions in the complex plane rather than a Breit-Wigner parametrization, shows two P_{11} poles: $P_{11}(\mathrm{I})=(1359,-100i)$ MeV and $P_{11}(\mathrm{II})=(1410,-80i)$ MeV. The KH and CMU-LBL PWA's do not indicate such a split.

A series of experiments has been performed by this collaboration over the last ten years to provide a complete set of πN scattering data in the region of the first two resonances, the $\Delta(1232)$-P_{33} and $N(1440)$-P_{11}(Roper). This series marks the first time that a complete set of measure-

©1989 The American Physical Society

ments has been made in any momentum region for the πN system. The measurements have been performed at the same accelerator, at the same momenta, and using the same beam channel. The set therefore precludes problems involving interpolation between data taken at different momenta using pion beams of different characteristics. Such interpolations, which can lead to large systematic uncertainties, have plagued all three PWA's.

Measurements of the differential cross section and the analyzing power for π^+p and π^-p elastic scattering and for $\pi^-p \to \pi^0 n$ have been reported.[19–23] Preliminary values of the spin-rotation parameters for π^+p and π^-p elastic scattering have also been presented.[24]

In the experiment described here, the recoil-proton polarization was measured for πp elastic scattering from unpolarized hydrogen. The momenta and angles chosen complement the measurements of the analyzing power previously made by this group and help to distinguish among predictions made by the three different PWA's.

II. NOTATIONS AND CONVENTIONS

The recoil polarization can be measured by rescattering the proton from a material whose analyzing power is known (such as carbon). The differential cross section for proton-carbon scattering is

$$\frac{d\sigma}{d\Omega}(\theta,\phi) \equiv I(\theta,\phi) = I_0(\theta)[1 + A_C(\theta)\mathbf{P}_r \cdot \hat{\mathbf{n}}] , \quad (1)$$

where I_0 is the unpolarized differential cross section, A_C is the analyzing power of carbon, $\hat{\mathbf{n}}$ is the unit normal to the rescattering plane, $\mathbf{P}_r$ is the polarization of the recoil proton, θ is the polar scattering angle, and ϕ is the azimuthal scattering angle (defined to be equal to zero when the plane defining the rescattering event is the same as the plane defining the original scattering event).

If the original scattering plane is defined to be the x-z plane, the normal to the rescattering plane can be written in terms of ϕ as

$$\hat{\mathbf{n}} = (-\sin\phi, \cos\phi, 0) ; \quad (2)$$

substitution into Eq. (1) yields

$$I = I_0(1 - A_C P_{rx} \sin\phi + A_C P_{ry} \cos\phi) . \quad (3)$$

Invariance under parity transformation requires that the polarization of a proton scattered from an unpolarized target be transverse to the scattering plane[25] so that Eq. (3) becomes

$$I = I_0(1 + A_C P_{ry} \cos\phi) . \quad (4)$$

The polarization can be written as

$$P_{ry} = \epsilon_{LR} / A_C , \quad (5)$$

where ϵ_{LR} is the asymmetry between scattering to the left ($\phi = 0$) and scattering to the right ($\phi = \pi$), and the differential cross section then becomes

$$I = I_0(1 + \epsilon_{LR} \cos\phi) . \quad (6)$$

If the recoil-proton polarization did contain components in the plane of the first scatter, then Eq. (3) would be modified to

$$I = I_0(1 + \epsilon_{UD} \sin\phi + \epsilon_{LR} \cos\phi) , \quad (7)$$

where ϵ_{UD} is the up-down asymmetry:

$$P_{rx} = -\epsilon_{UD} / A_C . \quad (8)$$

If the azimuthal scattering angle is measured for each good event, the left-right and up-down asymmetries can be determined by performing a Fourier analysis on the set of events using Eq. (7). If the analyzing power of carbon is known, the polarization of the recoil proton can then be calculated from Eqs. (5) and (8).

Since the recoil-proton polarization does not contain components in the original scattering plane, the up-down asymmetry must be equal to zero. A measurement of this quantity provides a check on systematic errors.

III. EXPERIMENT

The measurements were performed in the P^3E channel of the Clinton P. Anderson Meson Physics Facility (LAMPF). Details of the channel characteristics can be found in Ref. 26. A summary of the pion beam characteristics for this experiment is given in Table I. An extra quadrupole doublet and two steering magnets were recently added to the end of the beam line; the final focusing done by these magnets helped provide a small beam spot at the target at higher intensities than those possible before their installation.

The layout of the experimental setup is shown in Fig. 1. The incident pion was scattered from a cylindrical liquid-hydrogen (LH_2) target 5.7 cm in diameter by 10 cm high. The large-acceptance spectrometer (LAS) was used to identify and analyze the momentum of the pion after scattering, and the recoil proton was detected and its polarization measured by the JANUS polarimeter. Two particle telescopes and a beam hodoscope were used to monitor beam fluctuations.

In order to check for systematic errors, it was desirable to have at least one set of measurements in which JANUS was placed at the same angle on either side of the beam line. Because the LAS could not be moved to the positions necessary to take measurements on the left side of the beam, a set of measurements performed for π^+ at an incident pion beam energy of 547 MeV/c used a two-scintillation pion telescope in place of the LAS. The telescope and JANUS were then switched to the side of the beam line opposite to their original positions midway into the collection of this data set. Data were also taken with the LAS at the same beam momentum for comparison purposes.

TABLE I. Pion-beam characteristics.

Beam momentum (MeV/c)	Beam polarity	Rate (10^7 π/s)	$\Delta p/p$ (%)	Spot size (cm)
547	$-$	1.0	1.0	1.5×2.5
547	$+$	10.0	1.0	1.5×2.0
625	$-$	0.4	2.0–3.0	1.0×2.0
625	$+$	3.0	3.0	1.0×1.5

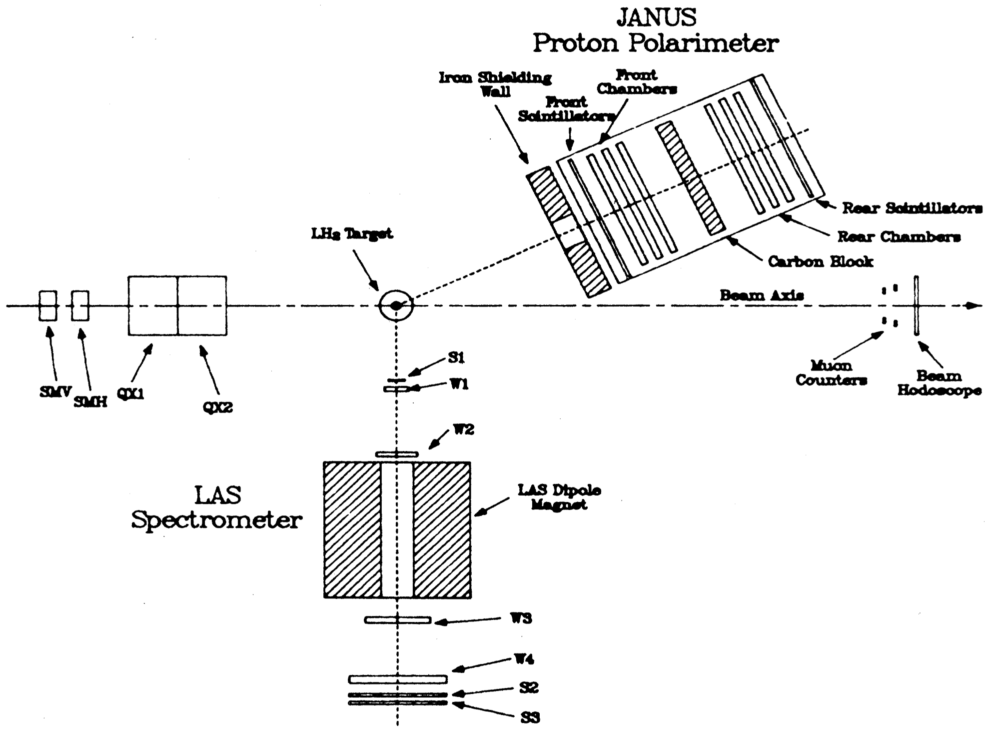

FIG. 1. Layout of the experimental setup (not to scale). SMV and SMH are vertical and horizontal steering magnets, respectively, while QX1 and QX2 are quadrupole magnets. S1 denotes the front scintillation counter on the LAS while S2 and S3 denote the rear scintillator planes. W1, W2, W3, and W4 denote the spectrometer's wire chambers.

A. The LAS and pion telescope

The LAS consisted of a dipole bending magnet sandwiched between four sets of multiwire proportional chambers (MWPC's). For this experiment, the quadrupoles of the LAS were removed and the dipole was pushed forward. The bend plane was vertical, with a nominal bend of 30°. All chambers had delay-line readouts. The wire spacing was 2 mm for all wire-chamber planes except $4X$, which was 4 mm.

A front scintillation counter and two scintillator planes (each composed of five overlapping counters) in the back provided time-of-flight and pulse-height information. Coincidence between the front scintillator and the back scintillator planes was used to signal that an event occurred in the LAS. Details about the LAS can be found in Ref. 27.

The pion telescope used for the measurements performed at 547 MeV/c consisted of the front LAS scintillator counter in coincidence with a second scintillation counter placed 60 cm behind.

B. The JANUS polarimeter

The JANUS polarimeter consisted of a front scintillator plane, three multiwire drift chambers, a carbon analyzer, three more identical chambers, and a back scintillator plane. The three chambers in front provided proton track information before the carbon analyzer while the three rear chambers provided track information after the proton had been rescattered from the carbon. An iron shielding wall with a hole matching the acceptance of the LAS was installed in front of JANUS to reduce the background in the chambers. Details about JANUS can be found in Ref. 28. Coincidence between front and back scintillator planes signaled an event in JANUS.

IV. DATA ANALYSIS

The overall event trigger for the experiment was a coincidence signal between the scintillators on the LAS (or the pion telescope) and the JANUS polarimeter. All events triggered in this manner were recorded. A series of tests was placed on these events in order to eliminate background.

(1) The time difference between the front scintillator of the LAS (or the pion telescope) and the front scintillator plane of JANUS and time-of-flight between the front scintillator of the LAS (or the pion telescope) and the rear scintillator planes of the LAS (or rear scintillator of the telescope) were recorded. Both spectra showed sharp, well-defined peaks; a narrow cut on these peaks provided good background rejection.

(2) Scattered pion momentum was determined from pion track information provided by the wire chambers in front of and in back of the dipole magnet of the LAS. The momentum spectrum provided a clean signal on

which to separate good events from background. This test was not available for runs with the pion telescope.

(3) Target projections from both the LAS and JANUS were calculated. Track information provided by the front chambers of both the spectrometer and the polarimeter were extrapolated back to the target to provide a "picture" of the target from both detectors. Only events emanating from the projected target were accepted for analysis. A target projection was not possible for the pion telescope. For this set of runs, therefore, only the projection from the polarimeter could be used.

Those events that passed all of the above tests were required to pass another set that was designed to select events that usefully rescattered in the polarimeter.

(1) An event was required to be detected in at least two of the three x and y planes upstream (two in front x and two in front y) and downstream (two in back x and two in back y) of the carbon analyzer. This increased the overall number of good events by approximately one-third over analyses that required all chamber planes.

During the experiment, it was discovered that two wires in chamber plane $Y5$ had broken their connection to the delay line and were not responding. Failure to account for events which should have triggered $Y5$ and either $Y4$ or $Y6$ near the two nonresponding wires in $Y5$ could cause systematic uncertainties. To check for this possibility, an analysis was done for three data points in which $Y5$ was completely disregarded. The results from this analysis were within 0.03 of the results from the standard analysis; since these differences are well within the statistical errors, any induced systematic error was small.

(2) For events in which all three chamber x or y planes in a set detected the recoil proton, the position of the proton in each chamber was checked by calculating the difference between the average proton position in the three chamber planes and the position in the middle chamber plane. If the result was greater than 1 mm, the event was rejected. The analysis required that the proton be detected in all three chamber planes for at least one of the four sets.

(3) For each event that passed the above tests, the distance of closest approach between a proton track into the carbon and one out of the carbon was calculated. A cut of 5 mm was placed on this distance (LAMPF, TRIUMF, and SIN use 5 mm as a convention[29]). Cuts were also placed on the x, y, and z coordinates of the midpoint of a line connecting the two tracks at the distance of closest approach to ensure that only events scattering within the carbon would be allowed.

(4) The polar scattering angle is sharply peaked at small angles due to multiple Coulomb scattering. Since these scattering events lower the analyzing power and have a large uncertainty in the azimuthal scattering angle, it is desirable to reject them, and a cut was therefore placed on $\sin\theta$. The values of the analyzing power for various values of $\sin\theta$ at 625 MeV/c are given in Table II. For each momentum, cuts were placed at the point where the analyzing power dropped below 0.4 (for consistency, a cut was also placed at large scattering angles where the analyzing power dropped below 0.4). This cut rejected 95–98 % of the recorded events. The thickness of the carbon analyzer used throughout the experiment was 6.3 cm, which was a compromise between the multiple-scattering angle and the need for a large number of nuclear scatters.

TABLE II. Analyzing power of carbon vs angle for 625 MeV/c.

θ_C (deg)	$\sin\theta_C$	A_C
3.13	0.06	0.21±0.006
3.68	0.06	0.25±0.007
4.29	0.08	0.29±0.01
5.19	0.09	0.35±0.01
	Cut	
6.32	0.11	0.43±0.01
7.45	0.13	0.50±0.01
8.63	0.15	0.57±0.02
9.81	0.17	0.61±0.02
11.25	0.20	0.64±0.02
13.26	0.23	0.60±0.02
15.84	0.27	0.50±0.02
	Cut	
18.35	0.31	0.38±0.01

(5) For each rescattering event with a given θ and ϕ, both the angle ϕ and $\phi+\pi$ were required to be within the acceptance of the polarimeter. This is done to avoid a systematic error owing to the finite size of the chambers. Using track information and the azimuthal scattering angle ϕ, the x and y positions of the proton at the back scintillator plane were calculated for each event. A similar calculation was performed for a track with an angle of $\phi+\pi$. If the $\phi+\pi$ track fell outside of the acceptance of the scintillator plane, the event was rejected.

To determine the recoil-proton polarization, the carbon analyzing power had to be determined from the data set provided by measurements performed at LAMPF, (Ref. 29) TRIUMF (Ref. 30), and SIN (Ref. 31). To make use of this data set, the analyzing power was parametrized as a function of proton energy and angle. Details of the parametrization used can be found in Ref. 29. The energy of the proton at the center of the analyzer, E_C, was determined using two-body kinematics and was corrected for the energy loss of the proton through half of the carbon.

V. CALCULATION OF THE POLARIZATION

As mentioned in Sec. II, the left-right and up-down asymmetries can be determined from Eq. (7) by using Fourier analysis. In order to do so, however, the only events that could have been used were ones which, for a given polar scattering angle θ, had all possible azimuthal scattering angles ϕ within the acceptance of the polarimeter. Since most events were already rejected because they did not usefully rescatter in the carbon, it was desirable to retain as many of the remaining events as possible and another method was used. This method only required the

$\phi+\pi$ acceptance criteria mentioned in Sec. IV and is developed in Ref. 32.

A series of data runs were made for each angle at each momentum. For each good event, the scattering angles were determined from the track information provided by the polarimeter drift chambers. The results were divided into twelve separate bins according to θ. (Some of the bins with small θ were excluded by the $\sin\theta$ cut, so the number of bins used in the analysis varied for each data point.)

The left-right and up-down asymmetries were then determined for each θ bin. The analyzing power of carbon was determined for the center of each bin using E_C and θ. The components of the polarization transverse to the scattering plane and in the scattering plane were then calculated by taking a weighted average of the results from the individual bins.

In order to provide a check on the analysis, polarizations were also calculated for each individual run at a particular momentum. These results were then compared to the result obtained from the analysis using all of the runs at that momentum. If the value of the polarization using all of the runs is assumed to be the true value of the polarization, an effective χ^2 can be defined as

$$\chi_r^2=\frac{1}{N_r}\sum_{i=1}^{N_r}\frac{(P_{ri}-P_f)^2}{\sigma_{ri}^2}\ , \tag{9}$$

where P_{ri} and σ_{ri} are the polarization and standard deviation calculated for each individual run, N_r is the number of individual runs, and P_f is the polarization calculated using all of the runs. A similar quantity can be defined in order to compare the results for each θ bin to the final result

$$\chi_\theta^2=\frac{1}{N_\theta}\sum_{i=1}^{N_\theta}\frac{(P_{\theta i}-P_f)^2}{\sigma_{\theta i}^2}\ , \tag{10}$$

where $P_{\theta i}$ and $\sigma_{\theta i}$ are the polarization and standard deviation for each individual bin and N_θ is the number of bins. The size of χ_r^2 and χ_θ^2 give an indication of the consistency of the analysis.

VI. RESULTS

The results obtained from Eqs. (9) and (10) are shown in Table III along with the results for both the transverse and in-plane polarizations. With one exception the χ^2 values indicate a very high degree of consistency both between the individual data runs and between the θ bins. The larger values of χ^2 obtained for π^+ at 625 MeV/c are due to the fact that the π^+p cross section at this angle and momentum is at a minimum resulting in measurements with lower statistics and larger overall background. Even so, the consistency between these runs is still acceptable. The results shown for the in-plane polarization using the up-down asymmetry are consistent with zero and therefore indicate that the systematic uncertainty is much smaller than the statistical uncertainty.

A more detailed presentation of the results for the transverse polarization obtained for π^+p elastic scattering at 547 MeV/c is given in Table IV. This table shows the result obtained by using the LAS and JANUS, the result obtained by using the pion telescope and JANUS, and the result obtained by placing the pion telescope and JANUS at the same angles but on opposite sides of the beam from their original positions. All three measurements show excellent agreement and again indicate a small systematic uncertainty.

These results, combined with the consistency of individual data runs and different θ bins and the fact that measurements of the up-down asymmetry were consistent with zero, indicate that systematic uncertainties were much smaller than statistical uncertainties. Therefore, the errors quoted are only statistical in nature.

Because of the large angular acceptance of the experimental apparatus (approximately 6° at the middle of the

TABLE III. Results.

Transverse polarization							
Momentum (MeV/c)	Beam polarity	$\cos\theta_{\mathrm{c.m.}}$	N_r	χ_r^2	N_θ	χ_θ^2	P
547	−	−0.50	8	1.4	8	0.9	0.98±0.04
547	+	−0.26	13	1.1	7	1.0	0.00±0.03
625	+	−0.43	7	0.9	7	2.1	0.82±0.06
625	−	−0.52	4	1.4	8	0.8	0.74±0.08
625	+	−0.52	5	2.4	7	4.6	−0.94±0.05

In-plane polarization							
Momentum (MeV/c)	Beam polarity	$\cos\theta_{\mathrm{c.m.}}$	N_r	χ_r^2	N_θ	χ_θ^2	P
547	−	−0.50	8	0.3	8	0.5	−0.03±0.05
547	+	−0.26	13	0.3	7	0.5	−0.08±0.03
625	−	−0.43	7	0.6	7	1.0	0.09±0.07
625	−	−0.52	4	0.6	8	0.4	0.04±0.08
625	+	−0.52	5	1.0	7	2.0	−0.07±0.06

TABLE IV. Comparison of runs at 547-MeV/c π^+.

	P
With LAS	-0.01 ± 0.03
With pion telescope	0.00 ± 0.03
JANUS & telescope switched	0.01 ± 0.04

carbon analyzer in JANUS) the results may be divided into two separate angular bins. These results, shown in Table V, show a smooth behavior of P with angle and help to map out the angular distributions near regions of interest, such as peaks or dips (the fact that the average P over the two angles is not exactly equal to P at one angle is a binning effect that caused slightly different good event samples in this analysis).

A. Comparison to previous measurements

The results of Table V are presented graphically in Fig. 2, together with this group's previous measurements of the analyzing power (Mokhtari *et al.*[21]) and the polarization measurements of Bareyre *et al.*[33,34]

Although a lack of overlapping data points precludes a precise comparison of the data of Bareyre *et al.* to the data from this experiment, Fig. 2 shows reasonable agreement between the two sets of 547 MeV/c. The results of Bareyre *et al.* at 617 MeV/c also show good qualitative agreement with those from this experiment at 625 MeV/c.

The results from the measurement of the analyzing power by Mokhtari *et al.* show good agreement at the points where the two measurements overlap (for π^+ at 625 MeV/c). The two experiments also show reasonable agreement elsewhere, with the exception of the measurement of Mokhtari *et al.* for $\cos\theta_{\mathrm{c.m.}}=-0.47$ at 547-MeV/c π^- which differ by 3σ. This measurement only used one arm in which only the protons were detected[21] and was therefore subject to a larger systematic uncertainty than the coincidence measurements.

B. Comparison to partial-wave analyses

Figure 3 shows the results of this experiment with those of the three partial-wave analyses discussed ear-

TABLE V. Results for the transverse polarization (more than one bin).

Beam momentum (MeV/c)	Beam polarity	$\cos\theta_{\mathrm{c.m.}}$	P
547	$-$	-0.48	0.99 ± 0.06
547	$-$	-0.51	1.03 ± 0.06
547	$+$	-0.25	0.00 ± 0.04
547	$+$	-0.27	0.00 ± 0.04
625	$-$	-0.42	0.89 ± 0.08
625	$-$	-0.45	0.77 ± 0.09
625	$-$	-0.50	0.79 ± 0.11
625	$-$	-0.53	0.66 ± 0.12
625	$+$	-0.50	-0.91 ± 0.08
625	$+$	-0.53	-0.93 ± 0.08

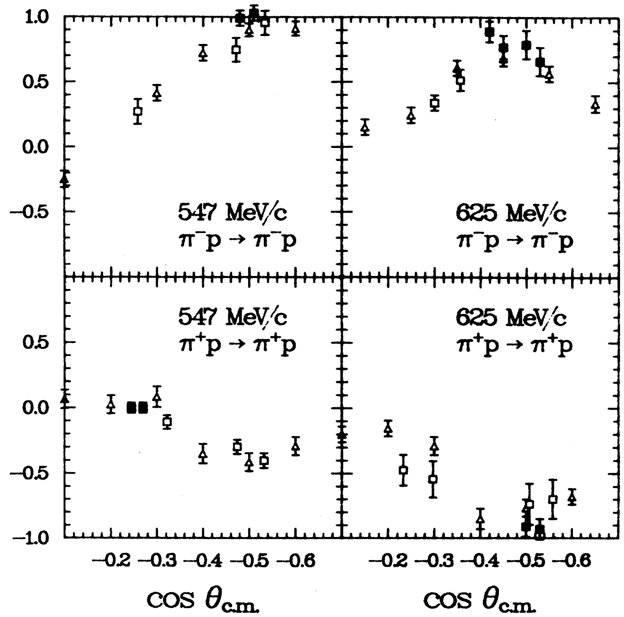

FIG. 2. Results of the present experiment at 547 and 625 MeV/c compared to the data of Mokhtari *et al.* (Ref. 21) at the same momenta and Bareyre *et al.* (Refs. 33 and 34) at 547 and 617 MeV/c. This experiment is represented by ■, Mokhtari *et al.* by □, and Bareyre *et al.* by △.

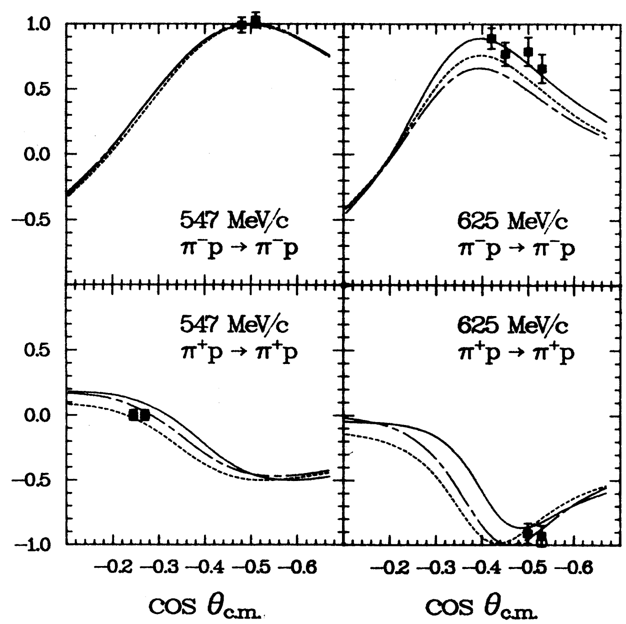

FIG. 3. Results of the present experiment at 547 and 625 MeV/c (■) compared to the results of the partial-wave analyses of CMU-LBL (dotted-dashed curve), KH (solid curve), and VPI (dashed curve).

lier.[16–18] Of the three analyses, only those of VPI contain the results of Mokhtari *et al.*

For 547-MeV/c π^-, all three analyses agree well to the results presented here. The π^+ results at 547 and 625 MeV/c agree with both the VPI and CMU-LBL solutions. The π^- results at 625 MeV/c favor the KH solution, although the VPI solution falls just outside one standard deviation.

The KH analysis has recently been updated to include more recent πN measurements, including those of Refs. 20–23. Preliminary results from this analysis agree, within the error bars, to all of the results contained here.[35]

VII. SUMMARY

Except at $\cos\theta_{\mathrm{c.m.}} = -0.47$ for 547-MeV/c π^-, the results presented here show reasonable agreement with the results obtained by Mokhtari *et al.* for the analyzing power. The single-arm measurement of the analyzing power performed at $\cos\theta_{\mathrm{c.m.}} = -0.47$ was subject to larger systematic uncertainties than his coincidence measurement, and the disagreement between it and the measurement of the recoil polarization indicates that the value obtained for A_n at this point should be used with caution.

Preliminary results from the updated KH analysis show slightly better agreement with the results presented here than does the VPI solution. However, a better judgement can be made only upon the completion of the analysis for the spin-rotation parameters and the incorporation of the data into both analyses.

The agreement between these measurements and the measurements of the analyzing power performed by Mokhtari *et al.* indicate that the systematic factors involved in both experiments are well understood.

ACKNOWLEDGMENTS

We gratefully acknowledge the support provided by LAMPF groups MP-7, MP-8, and MP-13 during the running of this experiment. We would especially like to thank M. McNaughton and K. H. McNaughton for their help with the JANUS polarimeter, P. A. M. Gram and J. C. Peng for their help with the LAS, and J. Novak and his group for providing the target. We would like to thank A. Bergmann for his help in the preliminary stages of this experiment. We are also grateful to G. Höhler for providing us with his preliminary partial-wave results. This work was supported in part by National Science Foundation Grants Nos. PHYS-8604524 and PHYS-8700306, the U.S. Department of Energy, and the Research Council at Abilene Christian University.

[1]T. Barnes and F. E. Close, Phys. Lett. **123B**, 89 (1983).
[2]J. D. Breit and C. R. Nappi, Phys. Rev. Lett. **53**, 889 (1984).
[3]K. C. Bowler and A. J. G. Hey, Phys. Lett. **69B**, 469 (1977).
[4]J. Carlson, J. B. Kogut, and V. R. Pandharipande, Phys. Rev. D **28**, 2807 (1983).
[5]A. Chodos, R. L. Jaffe, K. Johnson, C. B. Thorn, and V. F. Weisskopf, Phys. Rev. D **9**, 3471 (1974).
[6]F. E. Close and R. R. Horgan, Nucl. Phys. **B164**, 413 (1980).
[7]T. A. DeGrand and C. Rebbi, Phys. Rev. D **17**, 2358 (1978).
[8]A. De Rújula, H. Georgi, and S. L. Glashow, Phys. Rev. D **12**, 147 (1975).
[9]G. Eckart, A. Hayashi, and G. Holzwarth, Nucl. Phys. **A448**, 732 (1986).
[10]E. Golowich, E. Haqq, and G. Karl, Phys. Rev. D **28**, 160 (1983).
[11]A. Hayashi *et al.*, Phys. Lett. **147B**, 5 (1984).
[12]N. Isgur and G. Karl, Phys. Rev. D **19**, 2653 (1979).
[13]M. P. Mattis and M. Karliner, Phys. Rev. D **31**, 2833 (1985).
[14]Eric Umland, Ian Duck, and W. von Witsch, Phys. Rev. D **27**, 2678 (1983).
[15]N. W. Dean and P. Lee, Phys. Rev. D **5**, 2741 (1972).
[16]R. E. Cutkosky *et al.*, Phys. Rev. D **20**, 2804 (1979).
[17]G. H. Höhler, F. Kaiser, R. Koch, and E. Pietarinen, *Handbook of Pion-Nucleon Scattering* (Physics Data No. 12-1) (Fachinformationszentrum, Karlsruhe, 1979); *Pion-Nucleon Scattering Phenomenological Analyses* (Landolt-Bornstein, Vol. I/9b2) (Spinger, Berlin, 1983).
[18]R. A. Arndt, J. Ford, and L. D. Roper, Phys. Rev. D **32**, 1085 (1985).
[19]F. O. Borcherding, Ph.D. thesis, UCLA, 1982.
[20]G. J. Kim, Ph.D. thesis, UCLA, 1988.
[21]A. Mokhtari *et al.*, Phys. Rev. D **35**, 810 (1987).
[22]M. E. Sadler *et al.*, Phys. Rev. D **35**, 2718 (1987).
[23]J. A. Wightman *et al.*, Phys. Rev. D **38**, 3365 (1988).
[24]M. E. Sadler, in *Proceedings of the Conference on Physics with Light Mesons and the Second International Workshop on πN Physics*, Los Alamos, 1987, edited by W. R. Gibbs and B. M. K. Nefkens (LANL Report LA-1184-C, Los Alamos, 1987), p. 200; D. B. Barlow *et al.*, Phys. Rev. Lett. **62**, 1009 (1989).
[25]J. J. Sakurai, *Invariance Principles and Elementary Particle Physics* (Princeton University Press, Princeton, NJ, 1964).
[26]W. J. Briscoe *et al.*, Nucl. Instrum. Methods **197**, 277 (1982).
[27]E. Colton, Nucl. Instrum. Methods **178**, 95 (1980).
[28]R. D. Ransome *et al.*, Nucl. Instrum. Methods **201**, 309 (1982).
[29]M. W. McNaughton *et al.*, Nucl. Instrum. Methods **A241**, 435 (1985).
[30]G. Waters *et al.*, Nucl. Instrum. Methods **153**, 401 (1978).
[31]E. Aprile-Giboni *et al.*, Nucl. Instrum. Methods **215**, 147 (1983).
[32]D. Besset *et al.*, Nucl. Instrum. Methods **166**, 515 (1979).
[33]P. Bareyre *et al.*, Phys. Rev. Lett. **14**, 198 (1965).
[34]P. Bareyre *et al.*, Phys. Rev. Lett. **14**, 878 (1965).
[35]G. Höhler (private communication).